



THREE-DIMENSIONAL ANALYSIS ON SUBSIDENCE OF SHALLOW FOUNDATION RESTING ON LIQUEFIED GROUND

Yoshikazu KOBAYASHI¹, Ikuo TOWHATA²

SUMMARY

The three dimensional method that is presented in this paper is specialized for prediction of permanent deformation of ground induced by seismic liquefaction. This method is characterized by an assumption of lateral displacement modes that consists of a half and a quarter period of sinusoidal function and the modeling of liquefied subsoil as viscous fluid. A series of example analysis is carried out for a model that presumes subsidence of heavy footings into liquefied subsoil to check the feature of the presented method. Since these results, the possibility of that soil solidification to connect the footings reduces the subsidence of the footings into liquefied ground is suggested. The mitigative effect of sheet pile walls on deformation of liquefied ground is taken into account, and its mitigative effect is confirmed by the series of example analysis.

INTRODUCTION

Seismic liquefaction is one of the major disaster in geotechnical engineering. In the case of Philippine earthquake in 1990, numerous facilities and buildings in Dugpan City lost their serviceability due to large displacement of its foundations induced by loss of the strength and the stiffness of the liquefied ground, ACACIO[1]. There are two kinds of damage of structures on liquefied ground by earthquake. One of them is of the effect of inertia force by strong motion. This pattern could be traceable by conventional finite element analysis for liquefied ground based on solid mechanics. However, another type of damage that is caused by the loss of the strength and large distortion of the liquefied ground after complete liquefaction is difficult to reproduce by the analysis since this is large deformation problem and it is important to consider the influence of the geometric nonlinearity.

A two dimensional analytical method was presented by Towhata[2] for prediction of the ground deformation after complete liquefaction. However, the liquefied ground flow is affected by its three dimensional configuration, thus the extend of the method to three dimensional model is significant for the prediction. Therefore, a three dimensional numerical method is presented for the prediction of liquefied ground deformation after complete liquefaction in this paper. This method takes the effect of large deformation into account, thus the effect of geometric nonlinearity is properly considered. And the mitigative effect of soil solidification and sheet pile walls are implemented in this method and is investigated by a series of example analysis that is on the assumption of centrifuge tests on subsidence of heavy footing into liquefied ground.

¹ Research associate, Nihon University, Tokyo, Japan. E-mail: kobayasi@civil.cst.nihon-u.ac.jp

² Professor, The University of Tokyo, Tokyo, Japan. E-mail: towhata@geot.t.u-tokyo.ac.jp

PREDICTION OF GROUND FLOW DISPLACEMENT RELATED LIQUEFACTION

The discretized method is presented for prediction of ground flow induced by seismic liquefaction. This method assumes that liquefied ground behaves as viscous fluid due to the velocity dependant nature of the liquefied sand that was observed by past element tests and shaking table tests by Nishimura[3] and Towhata[4]. And the effect of inertia force by strong motion is omitted from this method due to the dominant component of driving force to liquefied ground during the strong motion is gravity force as indicated by shaking table test, Sasaki[5].

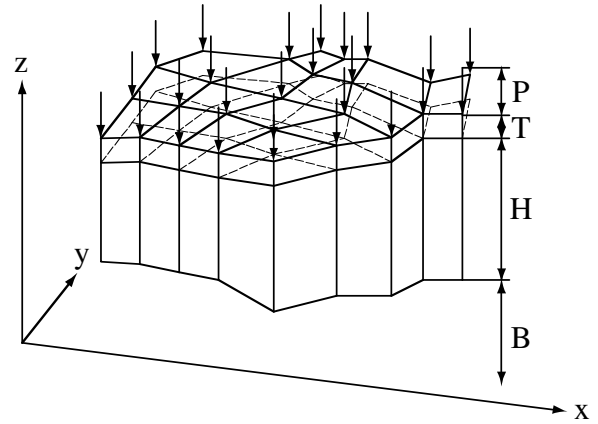


Fig.1 Model ground

Modeling of target ground

Liquefied ground is subdivided into column elements as illustrated in Fig.1. The elevation of the base, B , the thickness of liquefiable layer, H , the thickness of the unsaturated surface layer, T , and the magnitude of surcharge that includes the dead weight of the surface soil layer is interpolated by a first order linear interpolate function for horizontal coordinate x and y for each column element.

$$B = a_1x + a_2y + a_3xy + a_4 \quad (1)$$

$$H = b_1x + b_2y + b_3xy + b_4 \quad (2)$$

$$T = c_1x + c_2y + c_3xy + c_4 \quad (3)$$

$$P = d_1x + d_2y + d_3xy + d_4 \quad (4)$$

Each coefficient in these equations are determined by the specified B , H , T , P at each nodal points. The thickness B , H , T and the magnitude of surcharge P at nodal points are decided by existing investigation method such as the standard penetration test, effective stress analysis and others.

Lateral displacement of liquefied ground is defined as superimposition of two deformation modes that were found by shaking table tests, Mizutani[6], Toyota[7]. These modes are described as a quarter and half period of sinusoidal function that are illustrated in Fig.2. Hereafter, the quarter period mode and the half period mode are named F and J mode, respectively. If the lateral displacement of liquefied ground in x and y direction is independently grows up, the lateral displacement in x -direction, u , and y -direction, v are:

$$u(x, y, z, t) = F_u(x, y, t) \sin \frac{\pi(z-B)}{2H} + J_u(x, y, t) \sin \frac{\pi(z-B)}{H} \quad (5)$$

$$v(x, y, z, t) = F_v(x, y, t) \sin \frac{\pi(z-B)}{2H} + J_v(x, y, t) \sin \frac{\pi(z-B)}{H} \quad (6)$$

where $F_u(x, y, t)$, $J_u(x, y, t)$, $F_v(x, y, t)$, $J_v(x, y, t)$ denote maximum value of each deformation mode. Each of them are discretized on horizontal plane to reproduce the three dimensional variation of lateral displacement distribution.

$$F_u(x, y, t) = \sum N_i(x, y) F_{ui}(t) \quad (7)$$

$$J_u(x, y, t) = \sum N_i(x, y) J_{ui}(t) \quad (8)$$

$$F_v(x, y, t) = \sum N_i(x, y) F_{vi}(t) \quad (9)$$

$$J_v(x, y, t) = \sum N_i(x, y) J_{vi}(t) \quad (10)$$

where $N_i(x, y)$ is an interpolate function around nodal point i , and $F_{ui}(t)$, $J_{ui}(t)$, $F_{vi}(t)$, $J_{vi}(t)$ are $F_u(x, y, t)$, $J_u(x, y, t)$, $F_v(x, y, t)$, $J_v(x, y, t)$ at nodal point i .

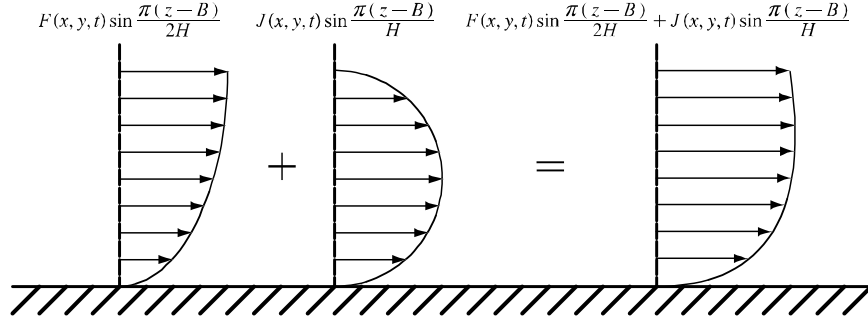


Fig.2 Deformation mode of liquefied ground

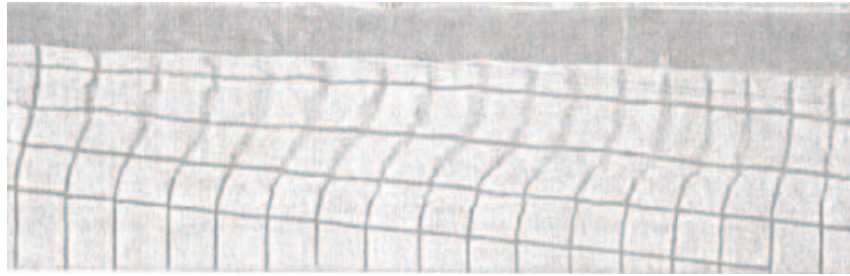


Fig.3 Liquefied sandy ground after shaking, Toyota[7]

Vertical displacement of liquefied ground is obtained from constant volume condition that is satisfied during liquefaction.

$$\frac{\partial u}{\partial x} + \frac{\partial v}{\partial y} + \frac{\partial w}{\partial z} = 0 \quad (11)$$

Thus, a differential equation is obtained by substituting lateral displacements of Eq.(5) and Eq.(6) to Eq.(11) for vertical displacement of liquefied ground.

$$\frac{\partial w}{\partial z} = \frac{\partial w_1}{\partial z} + \frac{\partial w_2}{\partial z} + \frac{\partial w_3}{\partial z} + \frac{\partial w_4}{\partial z} \quad (12)$$

$$\frac{\partial w_1}{\partial z} = -\frac{\partial F_u}{\partial x} \sin \frac{\pi(z-B)}{2H} - \frac{\partial J_u}{\partial x} \sin \frac{\pi(z-B)}{H} \quad (13)$$

$$\frac{\partial w_2}{\partial z} = \frac{\pi\{(a_1 + a_3 y)H + (b_1 + b_3 y)(z-B)\}}{H^2} \left\{ \frac{1}{2} F_u \cos \frac{\pi(z-B)}{2H} + J_u \cos \frac{\pi(z-B)}{H} \right\} \quad (14)$$

$$\frac{\partial w_3}{\partial z} = -\frac{\partial F_v}{\partial y} \sin \frac{\pi(z-B)}{2H} - \frac{\partial J_v}{\partial y} \sin \frac{\pi(z-B)}{H} \quad (15)$$

$$\frac{\partial w_4}{\partial z} = \frac{\pi\{(a_2 + a_3 x)H + (b_2 + b_3 x)(z-B)\}}{H^2} \left\{ \frac{1}{2} F_v \cos \frac{\pi(z-B)}{2H} + J_v \cos \frac{\pi(z-B)}{H} \right\} \quad (16)$$

Consequently, the vertical displacement of liquefied ground is given by solving Eq.(12) with boundary condition that vertical displacement is equal to zero at the bottom liquefiable layer, $z = B$.

Potential Energy, Kinetic energy and Dissipation energy of liquefied ground

The potential energy of liquefied ground is calculated in terms of $F_u(x, y, t)$, $J_u(x, y, t)$, $F_v(x, y, t)$, $J_v(x, y, t)$. Since the complete loss of the strength and stiffness of the liquefied subsoil, the strain energy

component of the potential energy is omitted for liquefied ground in this method. Therefore, only gravitational component of potential energy is taken into account.

Fig.3 shows the saturated sandy slope after shaking, Toyota[7]. This figure indicates that ground flow stopped when the ground surface is horizontal. This fact implies that the driving force varies with the deformation of liquefied ground and it reaches 0 when gravitational potential energy achieved the minimum state. This is the characteristic of geometric nonlinearity caused by large deformation, and the geometric nonlinearity should be taken into account for liquefied ground flow prediction.

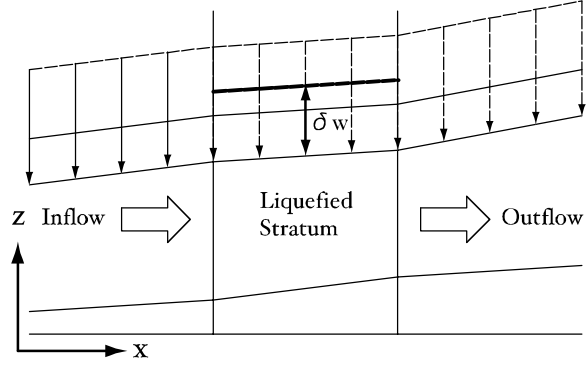


Fig.4 Elevation of ground surface

The variation of ground surface elevation is taken into account to consider the geometric nonlinearity. If the constant volume condition of a soil column element in liquefied ground is satisfied as indicated in Fig.4, the elevation of liquefied ground surface is calculated from lateral displacement of liquefied ground from the conservation of mass. The volume of inflow and outflow are obtained by the integration of lateral displacement of liquefied ground.

$$V_I = \int_B^{H+B} u(x, y, z, t) dz dy + \int_B^{H+B} v(x, y, z, t) dz dx \quad (17)$$

$$V_O = \int_B^{H+B} u(x + dx, y, z, t) dz dy + \int_B^{H+B} v(x, y + dy, z, t) dz dx \quad (18)$$

If the conservation of mass is satisfied, the difference between the volume of inflow and outflow is directly related with the variation of the ground surface δw as follows.

$$\begin{aligned} \delta w = \frac{V_I - V_O}{dx dy} = & \frac{\int_B^{H+B} u(x + dx, y, z, t) dz - \int_B^{H+B} u(x, y, z, t) dz}{dx} \\ & + \frac{\int_B^{H+B} v(x, y + dy, z, t) dz - \int_B^{H+B} v(x, y, z, t) dz}{dy} \end{aligned} \quad (19)$$

By considering the limiting value, δw is given by

$$\delta w = \lim_{\substack{dx \rightarrow 0 \\ dy \rightarrow 0}} \frac{V_I - V_O}{dx dy} = \frac{\partial}{\partial x} \int_B^{H+B} u(x, y, z, t) dz + \frac{\partial}{\partial y} \int_B^{H+B} v(x, y, z, t) dz \quad (20)$$

Consequently, the elevation of liquefied ground surface is calculated by substituting Eq.(5) and Eq.(6) to Eq.(20).

$$\delta w = -\delta w_1 - \delta w_2 - \delta w_3 - \delta w_4 \quad (21)$$

$$\delta w_1 = \frac{\partial}{\partial x} \int_B^{H+B} u(x, y, z, t) dz = -\frac{2H}{\pi} \left(\frac{\partial F_u}{\partial x} + \frac{\partial J_u}{\partial x} \right) - \frac{2(b_1 + b_3 y)}{\pi} (F_u + J_u) \quad (22)$$

$$\delta w_2 = \frac{\partial}{\partial x} \int_B^{H+B} v(x, y, z, t) dz = -\frac{2H}{\pi} \left(\frac{\partial F_v}{\partial x} + \frac{\partial J_v}{\partial x} \right) - \frac{2(b_1 + b_3 x)}{\pi} (F_v + J_v) \quad (23)$$

$$\delta w_3 = \frac{\partial}{\partial y} \int_B^{H+B} u(x, y, z, t) dz = -\frac{2H}{\pi} \left(\frac{\partial F_u}{\partial y} + \frac{\partial J_u}{\partial y} \right) - \frac{2(b_2 + b_3 x)}{\pi} (F_u + J_u) \quad (24)$$

$$\delta w_4 = \frac{\partial}{\partial y} \int_B^{H+B} v(x, y, z, t) dz = -\frac{2H}{\pi} \left(\frac{\partial F_v}{\partial y} + \frac{\partial J_v}{\partial y} \right) - \frac{2(b_2 + b_3 y)}{\pi} (F_v + J_v) \quad (25)$$

Due to the elevation of liquefied ground surface that was given as Eq.(21), the potential energy of liquefied ground P_l is obtained as follow.

$$P_l = \int_S \int_B^{H+B+\delta w} \rho_l g z dz ds \quad (26)$$

where ρ_l is the mass density of liquefied sand and g is gravity acceleration. If the variation of the gravitational potential energy is concentrated, the variation of the gravitational potential energy of liquefied ground is described as follow.

$$dP_l = \int_S \int_B^{H+B+\delta w} \rho_l g z dz ds - \int_S \int_B^{H+B} \rho_l g z dz ds = \int_S \int_{H+B}^{H+B+\delta w} \rho_l g z dz ds \quad (27)$$

Consequently, the variation of the gravitational potential energy dP_l is given by

$$dP_l = \int_S \int_{H+B}^{H+B+\delta w} \rho_l g z dz ds = \frac{1}{2} \int_S \rho_l g \{\delta w^2 + 2\delta w(H+B)\} ds \quad (28)$$

This is noteworthy that dP_l contains the variation of liquefied ground surface elevation and the geometric nonlinearity is taken into account. Because of this manner, the variation of driving force with deformation of liquefied ground is properly considered.

Kinetic energy of liquefied ground is obtained by conventional manner. Since the lateral and vertical displacement of liquefied subsoil are given, the kinetic energy of liquefied subsoil K_l is

$$K_l = \int_S \int_B^{H+B} \frac{1}{2} \rho_l (\dot{u}^2 + \dot{v}^2 + \dot{w}^2) dz ds \quad (29)$$

where s is the projection of target district on horizontal plane, and ρ_l is the mass density of liquefied subsoil as well.

Dissipation energy of liquefied ground is computed by modeling the liquefied subsoil as viscous fluid. Especially, since this method assumes the liquefied subsoil totally lose its strength and stiffness during ground flow, the liquefied subsoil is modeled as Newtonian fluid. Due to the stress tensor of Newtonian fluid is described as

$$\sigma_{ij} = \frac{1}{2} \left\{ \frac{\partial \dot{u}_i}{\partial x_j} + \frac{\partial \dot{u}_j}{\partial x_i} \right\} \quad (30)$$

where $u_1, u_2, u_3, x_1, x_2, x_3$ are correspond to u, v, w, x, y, w , the dissipation energy of liquefied ground D_l are obtained by

$$D_l = \int_S \int_B^{H+B} \mu \left\{ 4 \left(\frac{\partial \dot{u}}{\partial x} \right)^2 + 4 \left(\frac{\partial \dot{v}}{\partial y} \right)^2 + 4 \frac{\partial \dot{u}}{\partial x} \frac{\partial \dot{v}}{\partial y} + \left(\frac{\partial \dot{u}}{\partial z} \right)^2 + \left(\frac{\partial \dot{v}}{\partial z} \right)^2 + \left(\frac{\partial \dot{u}}{\partial y} + \frac{\partial \dot{v}}{\partial x} \right)^2 \right\} dz ds \quad (31)$$

where μ is viscosity coefficient of liquefied subsoil. It is note that the constant volume condition is applied to Eq.(30) for Eq.(31), and the component related with $\frac{\partial \dot{w}}{\partial x}$ and $\frac{\partial \dot{w}}{\partial y}$ are ignored since the

effect of these term is smaller than the others in case of real ground because the inclination of the real ground surface is only few percent in general, and the horizontal shear strain of liquefied ground is sometimes over 100 percent.

Governing Equation

Lagrange equation of motion is employed as a governing equation of motion.

$$\frac{d}{dt} \left\{ \frac{\partial L}{\partial \dot{q}_i} \right\} - \frac{\partial L}{\partial q_i} = - \frac{1}{2} \frac{\partial D}{\partial \dot{q}_i} \quad (32)$$

in which,

$$L = K - P \quad (33)$$

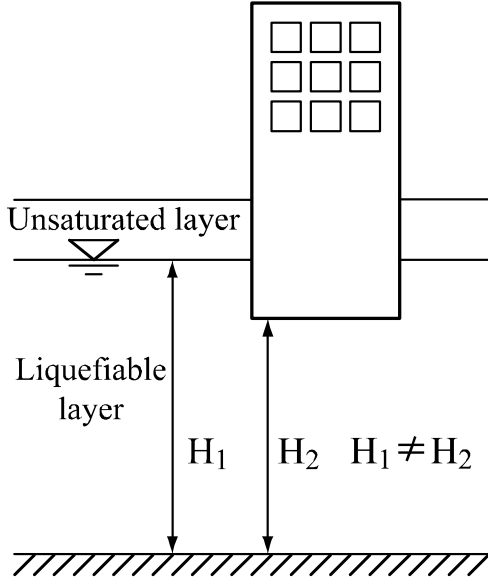


Fig.5 Discontinuity of the thickness of liquefiable layer

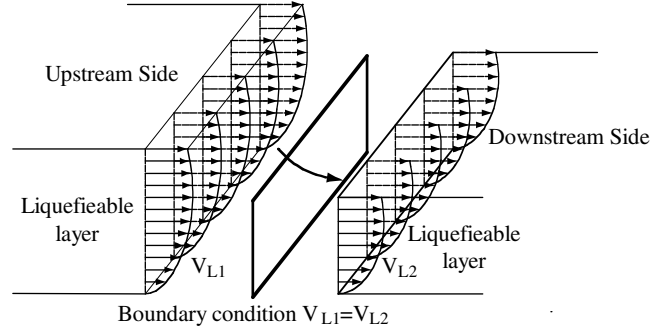


Fig.6 Discontinuous boundary

where K is kinetic energy, P is potential energy, q_i and \dot{q}_i are generalized displacement and velocity, respectively. These correspond to $F_{ui}(t)$, $J_{ui}(t)$, $F_{vi}(t)$, $J_{vi}(t)$, $\dot{F}_{ui}(t)$, $\dot{J}_{ui}(t)$, $\dot{F}_{vi}(t)$, $\dot{J}_{vi}(t)$ in this method. This method is characterized by the definition of lateral displacement of liquefied subsoil that is described as superimposition of two deformation mode of analytical functions, and the modeling of liquefied soil as Newtonian fluid. The number of degree of freedom is drastically reduced than typical three dimensional finite element analysis since nodal points is not required in vertical direction except ground surface. This characteristic contributes saving of computation time. The cost of ground investigation is also reduced because the constitutive equation of liquefied subsoil is simple, and consists of only viscosity of liquefied subsoil.

DISCONTINUOUS BOUNDARY

The definition of lateral displacement and geometric configuration of liquefied subsoil contribute saving of computational time as mentioned in previous section. However, on the other hand, these conditions require the continuity of the geometric configuration in liquefied ground. However, this condition is sometimes incompatible with a situation of real ground. For example, if a foundation is deeper than the thickness of unsaturated surface crust as illustrated in Fig.5, the thickness of liquefied layer is irregular around the structure.

Discontinuous boundary condition is presented to take the irregular into account by the conservation of mass. If the volume of flux is conserved between both side of the discontinuous boundary as illustrated in Fig.6, the following boundary condition is fulfilled.

$$V_{L1} - V_{L2} = 0 \quad (34)$$

in which,

$$V_{L1} = \int_l \int_B^{H+B} n \cdot U \, dz \, dl \quad (35)$$

$$V_{L2} = \int_l \int_B^{H+B} n \cdot U \, dz \, dl \quad (36)$$

$$U = \{u(x, y, z, t), v(x, y, z, t)\}^t \quad (37)$$

where V_{L1} and V_{L2} are the influx volume of liquefied subsoil from liquefied ground to discontinuous boundary and the efflux volume from discontinuous boundary to liquefied ground, and n is a normal vector to the discontinuous boundary as shown in Fig.7. Note that exchange of potential energy between the both side of the discontinuous boundary is automatically considered since the conservation of mass is fulfilled.

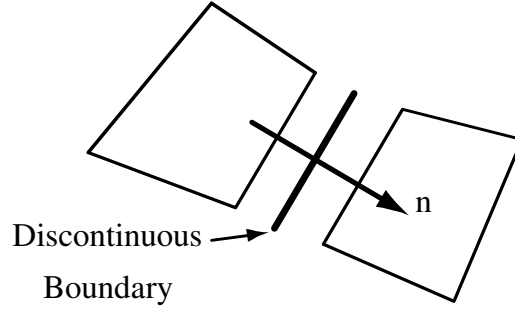


Fig.7 Vector n for discontinuous boundary

SHEETPILE WALL

Modeling of Sheet Pile Wall

Sheet pile wall is modeled as an elastic bending slab to take its mitigative effect into account. If the displacement of the sheet pile wall is given by ρ , the boundary condition between the sheet pile wall and, upstream and downstream side of liquefied sand are derived from the conservation of mass as well as discontinuous boundary condition as indicated in Fig.8.

$$B_1 = \xi_1 \left(\int_l \int_{B_1}^{H_1+B_1} n \cdot U_1 dz dl - \int_l \int_{B_1}^{H_1+B_1} \rho dz dl \right) \quad (38)$$

$$B_2 = \xi_2 \left(\int_l \int_{B_2}^{H_2+B_2} n \cdot U_2 dz dl - \int_l \int_{B_2}^{H_2+B_2} \rho dz dl \right) \quad (39)$$

where ξ_1 and ξ_2 are Lagrangian multipliers, n is a vector which direction is normal to the sheet pile wall. These boundary conditions reveal that the volume of influx from liquefied subsoil is the same with the volume of the void that is generated by the deformation of the sheet pile.

The strain energy of the sheet pile wall is given by the conventional theory of elastic beam.

$$E_s = \int_l \int_{B_1}^{H_1+B_1} \frac{1}{2} E_p I_p \left(\frac{\partial^2 \rho}{\partial z^2} \right)^2 dz dl \quad (40)$$

By substituting the functional that is given as the summation of the Lagrangian and boundary conditions that are described as Eq.(38) and Eq.(39) to Lagrangian equation of motion, the consequent equation is given by

$$\frac{\partial K_l}{\partial \ddot{q}_i} + \frac{1}{2} \frac{\partial D_l}{\partial \dot{q}_i} + \frac{\partial P_l}{\partial q_i} + \frac{\partial E_s}{\partial q_i} + \frac{\partial B_1}{\partial q_i} + \frac{\partial B_2}{\partial q_i} = 0 \quad (41)$$

For this equation of motion, ξ_1 , ξ_2 and ρ_j that are parameters to determine the shape of sheet pile wall deformation are appended to the list of the generalized displacement q_i to employ these boundary

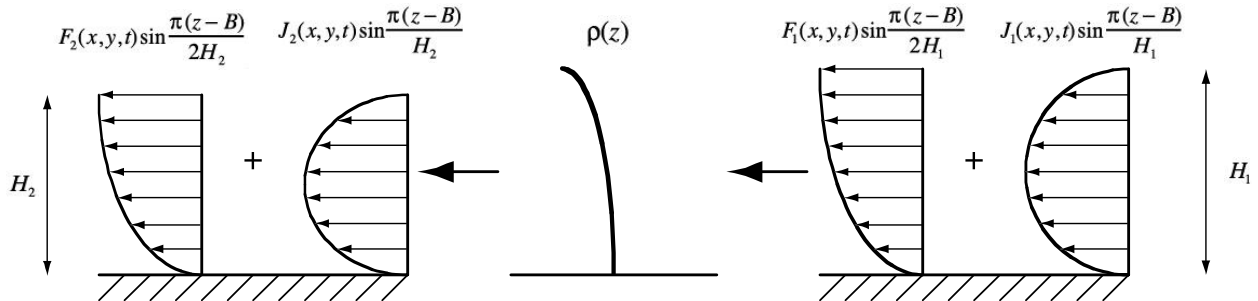


Fig.8 Boundary condition for sheet pile wall model

condition. Consequently, following equation is fulfilled during ground flow.

$$\frac{\partial K_l}{\partial \ddot{q}_i} + \frac{1}{2} \frac{\partial D_l}{\partial \dot{q}_i} + \frac{\partial P_l}{\partial q_i} + \xi_1 \frac{\partial \int_l \int_{B_1}^{H_1+B_1} n \cdot U_1 dz dl}{\partial q_i} + \xi_2 \frac{\partial \int_l \int_{B_2}^{H_2+B_2} n \cdot U_2 dz dl}{\partial q_i} = 0 \quad (42)$$

$$\frac{\partial B_1}{\partial \xi_1} = \int_l \int_{B_1}^{H_1+B_1} n \cdot U_1 dz dl - \int_l \int_{B_1}^{H_1+B_1} \rho dz dl = 0 \quad (43)$$

$$\frac{\partial B_2}{\partial \xi_2} = \int_l \int_{B_2}^{H_2+B_2} n \cdot U_2 dz dl - \int_l \int_{B_2}^{H_2+B_2} \rho dz dl = 0 \quad (45)$$

$$\frac{\partial E_s}{\partial \rho_j} + \frac{\partial B_1}{\partial \rho_j} + \frac{\partial B_2}{\partial \rho_j} = 0 \quad (46)$$

By substituting Eq.(38), Eq.(39) and Eq.(40) to Eq.(46),

$$\frac{\partial}{\partial \rho_j} \int_l \int_{B_1}^{H_1+B_1} \frac{1}{2} E_p I_p \left(\frac{\partial^2 \rho}{\partial z^2} \right)^2 dz dl - \frac{\partial}{\partial \rho_j} \int_l \int_{B_1}^{H_1+B_1} \xi_1 \rho dz dl - \frac{\partial}{\partial \rho_j} \int_l \int_{B_2}^{H_2+B_2} \xi_2 \rho dz dl = 0 \quad (47)$$

is obtained. This equation is developed by the integration by parts,

$$\int_l \left[E_p I_p \frac{\partial^2 \rho}{\partial z^2} \frac{\partial^2 \rho}{\partial z \partial \rho_j} \right]_{B_1}^{H_1+B_1} dl - \int_l \left[E_p I_p \frac{\partial^3 \rho}{\partial z^3} \frac{\partial \rho}{\partial \rho_j} \right]_{B_1}^{H_1+B_1} dl + \frac{\partial \rho}{\partial \rho_j} C_1 = 0 \quad (48)$$

is given as an equivalent boundary condition. For Eq.(48), following boundary condition is employed by the conventional theory of elastic beam.

$$\rho = 0 \quad \text{at} \quad z = B \quad (49)$$

$$\frac{\partial \rho}{\partial z} = 0 \quad \text{at} \quad z = B \quad (50)$$

$$\frac{\partial^2 \rho}{\partial z^2} = 0 \quad \text{at} \quad z = H + B \quad (51)$$

$$\frac{\partial^3 \rho}{\partial z^3} = 0 \quad \text{at} \quad z = H + B \quad (52)$$

Therefore,

$$C_1 = \int_l \int_{B_1}^{H_1+B_1} E_p I_p \frac{\partial^4 \rho}{\partial z^4} - \xi_1 - \frac{H_2}{H_1} \xi_2 dz dl = 0 \quad (53)$$

is satisfied during the ground flow induced by liquefaction. Consequently,

$$\frac{\partial^4 \rho}{\partial z^4} = \frac{1}{E_p I_p} \left(\xi_1 + \frac{H_2}{H_1} \xi_2 \right) \quad (54)$$

is fulfilled as a boundary condition. This reveals that the lateral earth pressure that acts on a sheet pile wall is taken into account as homogeneous lateral pressure. In this case, the deformation shape of sheet pile wall in liquefied ground flow is able to be determined by only one parameter, for example, ρ_m that is the displacement of the top of the sheet pile wall.

EXAMPLE ANALYSIS AND RESULTS

Simple element test

A series of example analysis for a simple model is carried out to check the mitigative effect of the sheet pile model. Fig.9 shows the model consists of two element, and a sheet pile wall is installed between the elements. The resultant deformation of the model is investigated by changing the bending stiffness of the

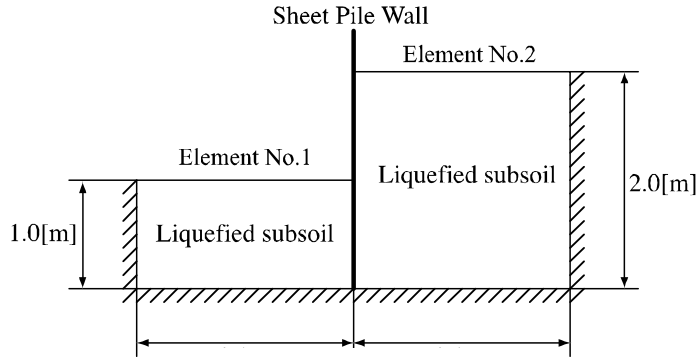


Fig.9 Simple Model

	EI[N·m ² /m]	H1[m]	H2[m]	μ [Pa·s]
Case1	200	2.0	1.00	5000
Case2	250	2.0	1.00	5000
Case3	300	2.0	1.00	5000
Case4	350	2.0	1.00	5000
Case5	200	2.0	1.25	5000
Case6	200	2.0	1.50	5000
Case7	200	2.0	2.00	5000
Case8	200	2.0	1.00	2500
Case9	200	2.0	1.00	7500
Case10	200	2.0	1.00	10000

Table.1 Material Parameters for Simple Model

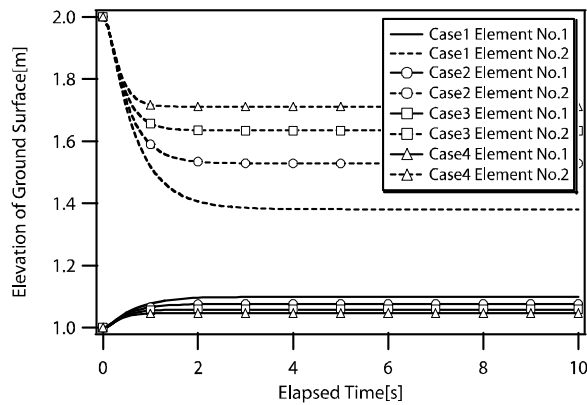


Fig.10 Elevation of ground surface of each element

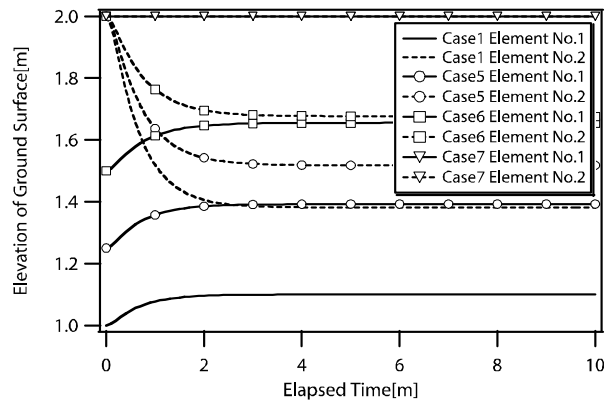


Fig.11 Elevation of ground surface of each element

sheet pile wall, the difference of initial elevation of ground surface and viscosity of liquefied sand as indicated in Table.1 for this model. Fig.10 compares the elevation of ground surface of element No.1 and No. 2 with Case 1, 2, 3 and 4 in which the stiffness of the sheet pile wall is changed. As shown in Fig.10, the elevation of the ground surface of the elements at ultimate equilibrium state varies with the bending stiffness of the sheet pile wall. This result is consistent with a common sense that stiffer sheet pile wall can reduce the lateral displacement of the liquefied ground more effectively. Fig.11 compares the resultant elevation of each element with Case 1, 5, 6, and 7 in which the difference of initial elevation of the ground surface is changed. This figure shows that deformation of the elements become smaller with the difference of initial elevation of each element, and the elements does not deform in Case 7 that the difference of initial elevation of each element is equal to zero since the lateral earth pressure that affects from both side to the sheet pile wall is balanced. Fig.12 compares the resultant elevation of ground surface of each element with Case 1, 8, 9, 10 in which the viscosity of liquefied sand is changed. According to Fig.12, the viscosity of liquefied subsoil affects the velocity of element deformation, however, it does not contribute to the deformation at the ultimate equilibrium.

Subsidence of separated footing

Fig. 13 shows a model of separated footings. This model is made on the assumption that centrifuge test was conducted, and this model has four separated shallow footings of 1.9[m] depth, the thickness of the liquefied layer is 17.5[m] in real scale. Fig. 14 illustrates numerical model for the model of separated footings that was illustrated in Fig.13. For this analysis, these footings are modeled as surcharge on the surface of liquefied ground. Equivalent mass that the weight of the mass is the same with the weight of

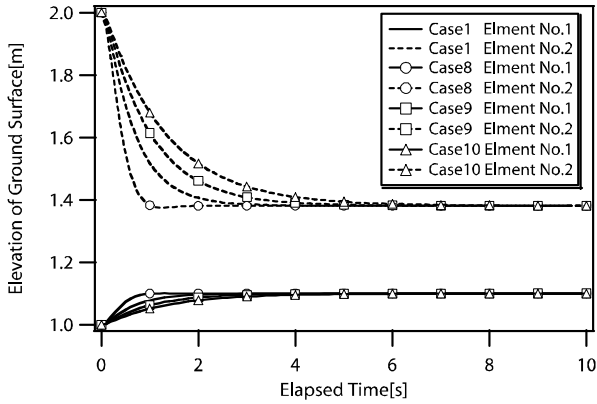


Fig.12 Elevation of ground surface of each element

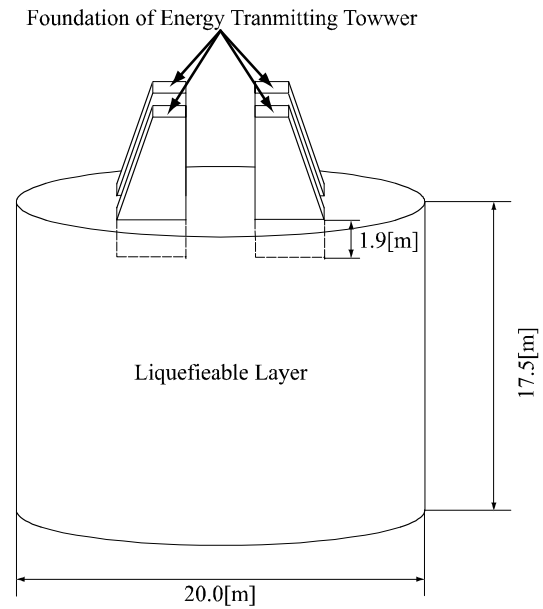


Fig.13 Target model

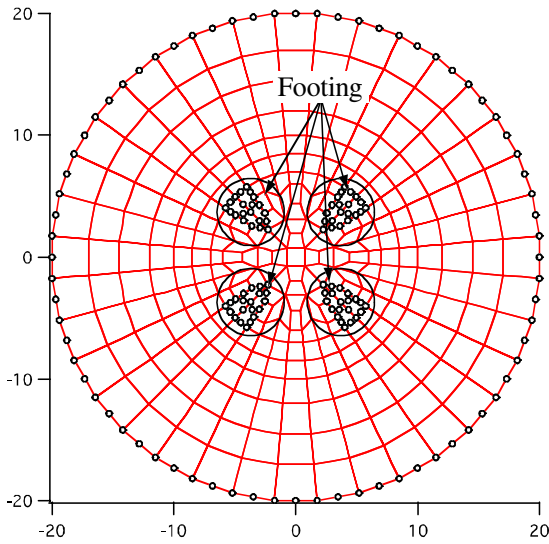


Fig.14 Numerical model for separated footings

Table.2 Material Property for the centrifuge model

	Mass Density[kg/m ³]	Viscosity[kPa · s]
Case1	1900	50000
Case2	1900	100000
Case3	1900	150000
Case4	1900	200000

the footings and tower is added to consider the inertia force of the footing and superstructure. Table. 2 shows the parameters that are employed for this analysis. The mass density of liquefied subsoil is decided as 1900[kg/m³] that is typical mass density of liquefied subsoil, and the viscosity of the liquefied subsoil was determined by referring to the results of element test, Chaminda[8]. The surcharge is calculated by assuming that the dead weight of a footings and superstructure is distributed homogeneously at the bottom of the footings. This is noteworthy that there is a discontinuity of the thickness of liquefiable layer between under the footings and the others. This discontinuity of the thickness of liquefiable layer is absorbed by discontinuous boundary condition that are presented in previous section. Fig.15 shows the time history of footing subsidence. It is note that the subsidence of each footing is the same in this model since this model is axi-symmetric for each footing as indicated in Fig.16. Therefore, one footing is picked up for investigation. According to Fig.15, the subsidence of the footing is extremely large in this case since the footing subsides until the buoyancy at the bottom of a footing is balance with the dead weight of the footing and tower. And the viscosity of liquefied subsoil contributes only the velocity of subsidence as well.

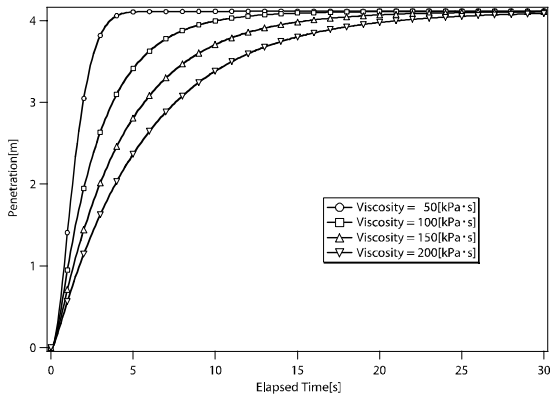


Fig.15 Time history of separated footing subsidence

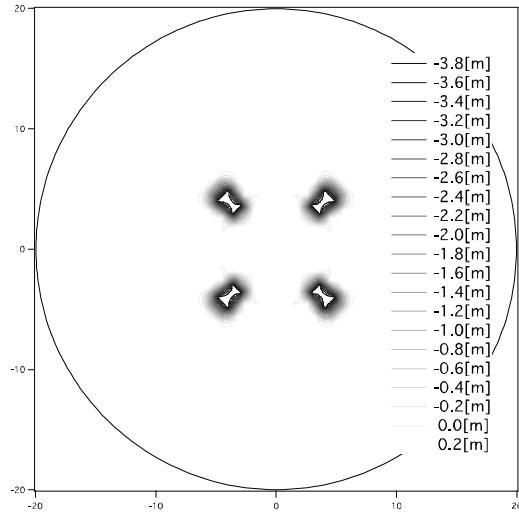


Fig.16 Contour of uplift of ground after 20[s]

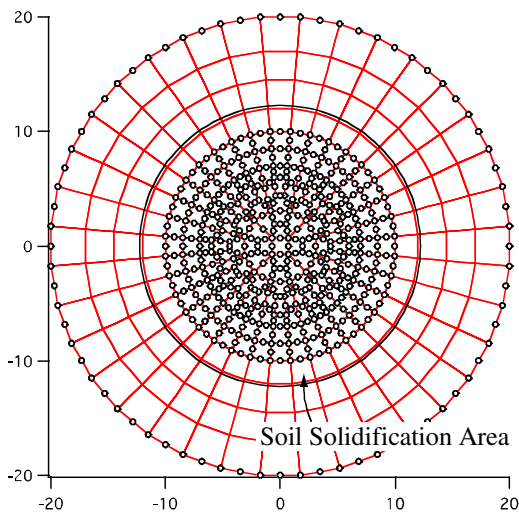


Fig.17 Numerical model for connected footing

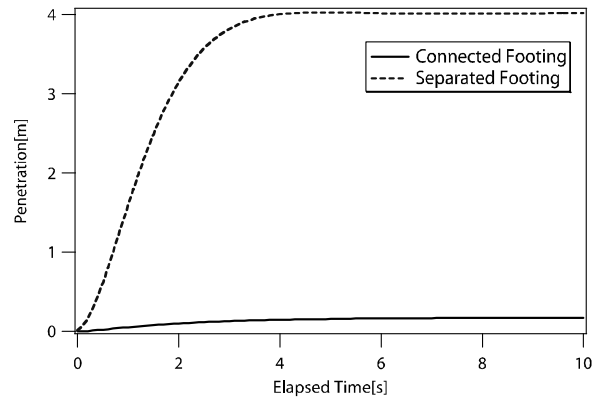


Fig.18 Comparison of separated footing and connected footing

Subsidence of connected footing

The deformation of liquefied ground is large deformation problem, and geometric nonlinearity is important for the prediction of the deformation as stated. In a previous section, the subsidence of the separated footing was investigated, and the equilibrium was achieved when the buoyancy is equal to the total dead weight of the footing and the tower. This result suggests that the subsidence is able to be reduced if the buoyancy per unit subsidence is increased. As a way to increase the buoyancy to the footing, the enlargement of the cross section of footing by soil solidification at the surface of liquefied ground which connects all footings is considered. Fig.17 shows the mesh for connected footing model. For this model, the circle area was defined for the area of ground improvement and it is assumed that the total weight of footings and tower is distributed homogeneously on the ground surface of the improved area. The equivalent mass is installed to consider the inertia force of footings, tower and soils that are solidification as well. Fig.18 compares the time history of the subsidence of the connected footing and the separated footing. According to Fig.18, the subsidence of the footings is drastically reduced by the soil

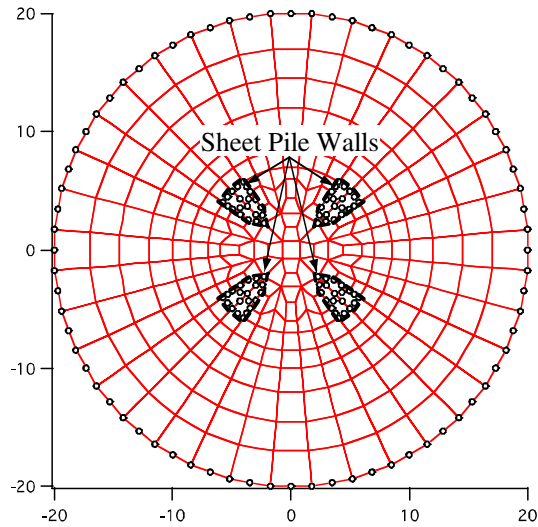


Fig.19 Numerical model for separated footing with sheet pile walls

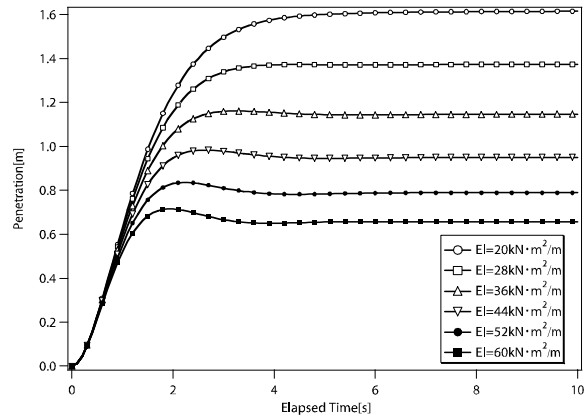


Fig.20 Comparison of subsidence of footing with various bending stiffness of sheet pile wall

solidification. The effect of the reduction of deformation depends on the extent of the soil solidification since large area soil solidification gives more buoyancy. This result indicates that the possibility of mitigation of damage that is caused by subsidence of the real structures induced by seismic liquefaction.

Subsidence of energy transmitting tower with sheet pile wall

Sheet pile wall is employed as another type of mitigation of the deformation of liquefied ground. The each footing are surrounded by embedded sheet pile walls that are presented in previous section as illustrated in Fig.19. For this model, the mitigative effect is investigated by changing the bending stiffness of the sheet pile walls. Fig.20 compares the time history of the subsidence of the footings. Fig.20 shows that the subsidence of the footings is prevented by the sheet pile walls, and the effect varies with the bending stiffness of the sheet pile wall.

CONCLUSIONS

The three dimensional numerical method for prediction of subsidence of structures that takes the effect of geometric nonlinearity into account was presented in this paper. This method was applied to a model of heavy footing on liquefied ground that is on assumption that centrifuge test was conducted, and the subsidence of the footing into liquefied ground was investigated. Two kinds of mitigation of liquefied ground deformation were investigated for the model. The result of the analysis that employs soil solidification as a mitigation of liquefied ground deformation suggests the possibility of that the subsidence of the footings is reduced by enlarging the cross section of the footings. The mitigative effect of sheet pile walls is considered by modeling the sheet pile wall as elastic beam, and the results of the analysis indicates the mitigative effect of the sheet pile walls.

REFERENCES

1. Alexis A. Acacio, Yoshikazu Kobayashi, Ikuo Towhata, R. Bautista and Kenji Ishihara. "Subsidence of building foundation resting upon liquefied subsoil; Case studies and assessment", Soils and Foundations, 2001, Vol.41 No.6, 111-128
2. Ikuo Towhata, Roland P. Orense, Hirofumi Toyota, "Mathematical principles in prediction of lateral ground displacement induced by seismic liquefaction", Soils and Foundations, 1999, Vol.39 No.2, 1-19

3. Satoshi Nishimura, Ikuo Towhata and Tsuyoshi Honda, "Laboratory shear tests on viscous nature of liquefied sand", *Soils and Foundations*, 2002, Vol.42 No.4, 89-98
4. I. Towhata, W. Vargas-Monge, R. P. Orense, M. Yao, "Shaking table tests on subgrade reaction of pipe embedded in sandy liquefied subsoil", *Soil Dynamics and Earthquake Engineering*, 1999, 18, 347-361
5. Yasushi Sasaki, Ikuo Towhata, Ken-Ichi Tokida, Kazuhiro Yamada, Hideo Matsumoto and Yukio Tamari, "Mechanism of permanent displacement of ground caused by seismic liquefaction", *Soils and Foundations*, 1992, Vol32 No.3, 79-96
6. Hirofumi Toyota, "Shaking table tests and analytical prediction on lateral flow of liquefied ground", Ph.D thesis, 1995, Department of Civil Engineering, School of Engineering, The University of Tokyo
7. Mizutani, T., Towhata, I., Shinkawa, N., Ibi, S., Komatsu, T., and Nagai, T., "Shaking table tests on mitigation of liquefaction-induced subsidence of river dikes", *Proc. 16th ICSMGE, Istanbul*, 2001, Vol2, 1207-1210
8. Chaminda. P. K. Gallge, "Laboratory shear tests on rate dependant nature of liquefied sand with fines", Master thesis, 2002, Department of Civil Engineering, The University of Tokyo